ACS Energy LETTERS

http://pubs.acs.org/journal/aelccp

Key Parameters in Determining the Reactivity of Lithium Metal Battery

Bingyu Lu, Diyi Cheng, Bhagath Sreenarayanan, Weikang Li, Bhargav Bhamwala, Wurigumula Bao,* and Ying Shirley Meng*

Cite This: *ACS Energy Lett.* 2023, 8, 3230−3238

Read Online

ACCESS | Metrics & More | Article Recommendations | Supporting Information

ABSTRACT: **Lithium metal anodes are crucial for high-energy-density batteries, but concerns regarding their safety remain. Limited investigations have evaluated the reactivity of Li metal anodes in full cell configurations. In this study, differential scanning calorimetry (DSC) and in situ Fourier-transform infrared spectroscopy (FTIR) were employed to quantitatively examine the Li metal reactivity. Lithiated graphite (Li-Gr) and lithiated silicon (Li-Si) were also compared. The reactivity of plated Li was systematically investigated when combined with different electrolyte compositions, morphologies, atmospheres, and various cathode materials (NMC622, LFP, and LNMO). It was discovered that all cell components, such as electrolyte composition, Li morphology, control of inactive Li accumulation, and cathode stability, play essential roles in regulating the reactivity of the plated Li. By optimizing these factors, the Li metal full cell exhibited no significant thermal reaction up to 400 °C. This research identifies key parameters for controlling Li metal reactivity, potentially advancing lithium metal battery design and manufacturing.**

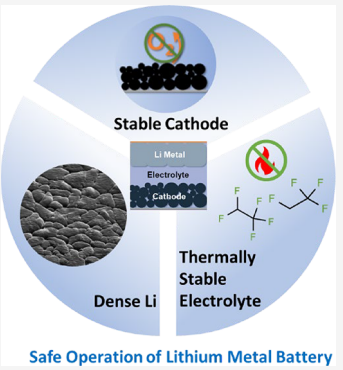

With the rapid growth in the demand of high-performance electric vehicles and personal portable devices, lithium (Li) metal has been a popular candidate as the anode material for developing high energy density rechargeable batteries (>500 Wh/kg) due to its high specific capacity (3,860 mAh/g) and low electrochemical potential (−3.04 V versus the standard hydrogen electrode).[1−3] Although extensive studies have been performed to prolong the cycle life of Li metal anode,[4−6] the potential safety hazard brought by metallic Li in the high energy density batteries is still one of the biggest obstacles before its large-scale commercialization.[7] The first attempt to commercialize Li metal cells in the 1980s ended in failure when multiple cases of cells catching on fire were reported.[8] Since then, the safety concerns of using Li metal as the anode material for high energy cells have never ceased.[9]

The safety hazards at the cell level are determined by the reactivity of each cell component and the interplay among them.[10] As for commercial Li-ion battery, there has been tremendous work studying the key factors in determining the reactivity of Li-Gr.[11−13] By utilizing accelerating rate calorimetry (ARC) and X-ray diffraction (XRD), Dahn et al. discovered that the lithiated graphite ($Li_{0.81}C_6$) starts to decompose with electrolyte at temperatures as low as 90 °C.[14] In situ synchrotron XRD and mass spectrometry (MS) were applied by Amine et al. to study the role of robust SEI in protecting lithiated graphite from thermal decomposition. Based on the current literature, it can be concluded that the lithiated graphite (Li-Gr) at the material level is far from a safe and stable material, but it can be implemented in state-of-the-art battery packs with proper engineering and optimizations.[15−17] As a highly reactive alkali metal, Li has always been considered unsafe for practical battery operations.[18,19] Various attempts have been made to design a safe rechargeable Li metal cell. In 1995, Aurbach and colleagues demonstrated an AA-size Li|LiMnO cell that can survive short-circuiting and overcharging tests. However, the authors also commented that cell safety is critically affected by the cycle numbers. Recently, novel electrolytes with nonflammable solvents have been proposed as ways to prevent the cell from catching on fire.[20−22] Fire-retarding localized high concentration electrolytes (LHCEs) have also been developed using nonflammable solvents or diluents, such as trimethyl phosphate or 2,2,2-trifluoroethyl-1,1,2,2-tetrafluoroethyl ether (HFE).[23,24] Recently, Yin and colleagues developed a new type of liquefied gas electrolyte with fire-extinguishing merit.[22] With the development of electrolytes, the Li metal anode is marching toward commercial reality with safe operation.

Received: May 21, 2023
Accepted: June 30, 2023

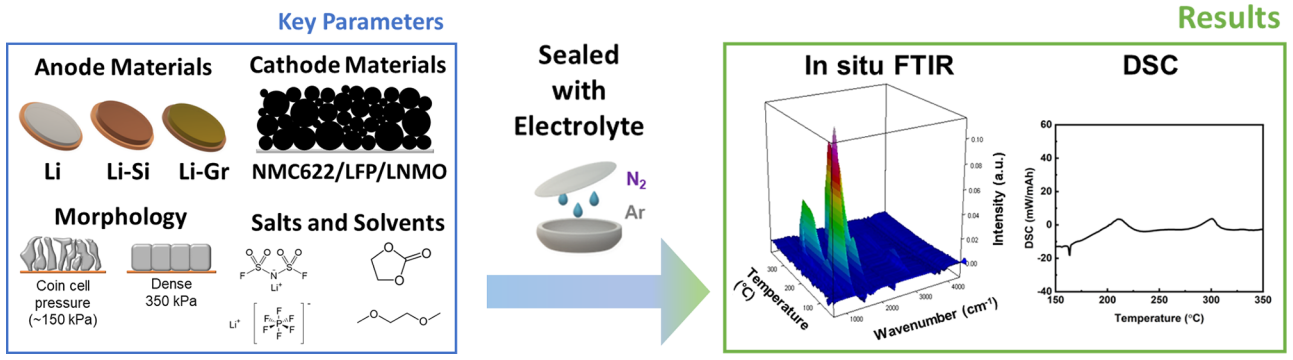

Figure 1. Schematics of the sample preparation and experimental process.

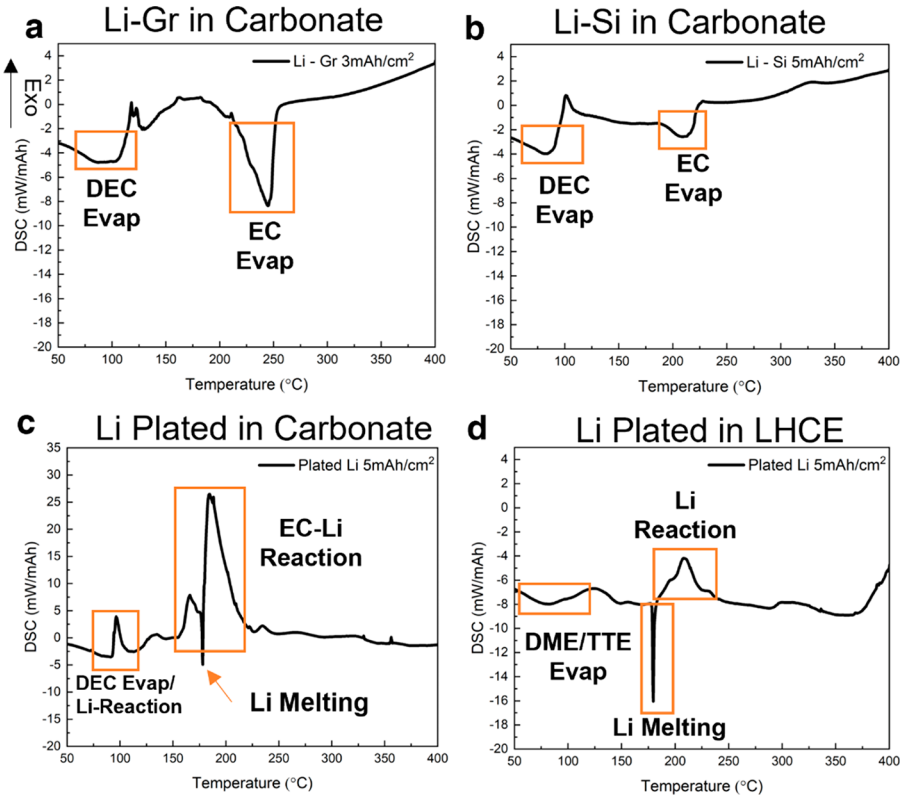

Figure 2. DSC curves of (a) Li-Gr, (b) Li-Si, (c) Li metal plated in carbonate, and (d) Li metal plated in LHCE. Graphite and Si anodes are lithiated to the desired capacity in half cell setup with the rate of C/20. Li metal is plated in Li|Cu coin cell to the desired capacity at a current density of 0.5 mA/cm^2.

Although these works have focused on preventing cells from catching on fire, it is still unclear how reactive Li metal is in nature, not to mention a direct comparison with other anode materials under a similar state of charge. It is commonly believed that pristine graphite and Si are much safer than Li metal when assembled in a cell. However, in practical applications, the battery is mainly in the charge state in which the anode is lithiated and its chemical stability is reduced significantly. Therefore, the reactivity of Li metal should be compared with those of Li-Gr and Li-Si, instead of the pristine ones. More work needs to be done to identify the key parameters in controlling the reactivity of Li metal in a battery system and provide design principles for a safe Li metal battery (LMB). There are multiple ways to define the metal reactivity under different cirtumstances.[25] For instance, a metal is considered highly reactive when (1) it causes large negative enthalpy of formation, ΔH_f, during a oxidation reaction, or (2) requires small sublimation energy and ionization energy during oxidation or hydration.[25] Since the anode at the charged state is full of electrons to be released, which can also react with water and oxygen violently,[6] it is important to *quantitatively* compare the reactivity of different anode materials in a well-controlled cell system.

Here, we quantitatively compare the reactivity of Li-Gr, Li-Si, and plated Li metal (plated-Li) in two different electrolytes by utilizing differential scanning calorimetry (DSC) coupled with in situ Fourier-transform infrared spectroscopy (FTIR). We further explored the effect of the Li morphology on the reactivity by precisely tuning the external stack pressure during the plating process. It was found that the thermal response of plated-Li metal in a well-designed system can be of the same magnitude as that of Li-Gr and Li-Si. Furthermore, the influence of the cathode on the Li metal reactivity is also

https://doi.org/10.1021/acsenergylett.3c01001
ACS Energy Lett. 2023, 8, 3230−3238

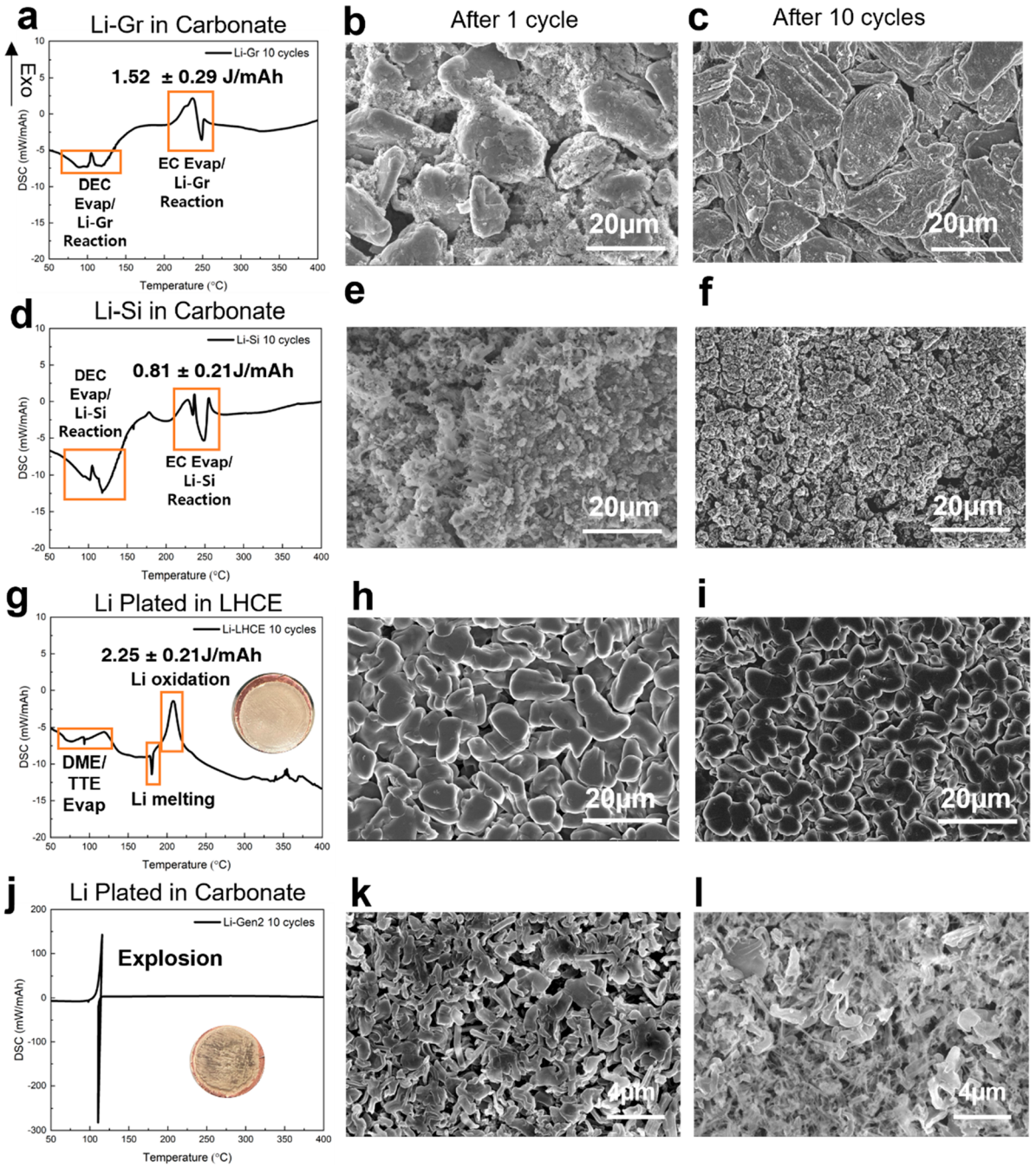

Figure 3. DSC curves of (a) Li-Gr, (d) Li-Si, (g) Li plated in LHCE, and (j) Li plated in carbonate after 10 cycles. The SEM images of anode morphology after 1 cycle and after 10 cycles: (b and c) graphite, (e and f) Si, (h and i) Li plated in LHCE, and (k–l) Li plated in carbonate. Insets: digital images of Li plated on the Cu after 10 cycles. The amount of heat released from the oxidation peak of each DSC curve is labeled in the corresponding figures. Graphite and Si anodes are cycled in half cell configuration at rate of C/20 and Li metal anodes are cycled in Li||Cu cells at rate of 0.5 mA/cm^2.

analyzed. Finally, a guideline for designing safer Li metal cells is provided.

Three anodes including Gr, Si, and bare Cu (no excess Li) were charged with a controlled lithiation/plating amount of 3 mAh/cm^2 for Gr or 5 mAh/cm^2 for Si and bare Cu in the half cell, as shown in Figure 1. Instead of 5 mAh/cm^2, 3 mAh/cm^2 capacity is chosen for the Gr because it is the most widely available capacity among commercialized Li-ion cells. The prepared anodes were sealed in a DSC pan with a controlled amount of electrolyte (E/C ratio ~3 mg/mAh) and then transferred into the DSD-FTIR station for thermal analysis. Detailed experimental designs can be found in the Supporting Information. All DSC tests are done at least twice to make sure that the obtained results are repeatable (Figure S5). Figure 2 shows the DSC curves of Li-Gr, Li-Si, and plated-Li in the carbonate-based electrolyte [carbonate, 1.2 M lithium hexafluorophosphate ($LiPF_6$) dissolved in ethylene carbonate (EC):diethyl carbonate (DEC) (1:1 by weight) with 10% fluoroethylene carbonate (FEC)]. In addition, plated-Li in LHCE [lithium bis(fluorosulfonyl)imide (LiFSI), 1,2-dimethoxyethane (DME), and 1,1,2,2-tetrafluoroethyl-2,2,3,3-Tetrafluoropropyl Ether (TTE) with molar ratio 1:1.2:3] was also

https://doi.org/10.1021/acsenergylett.3c01001
ACS Energy Lett. 2023, 8, 3230−3238

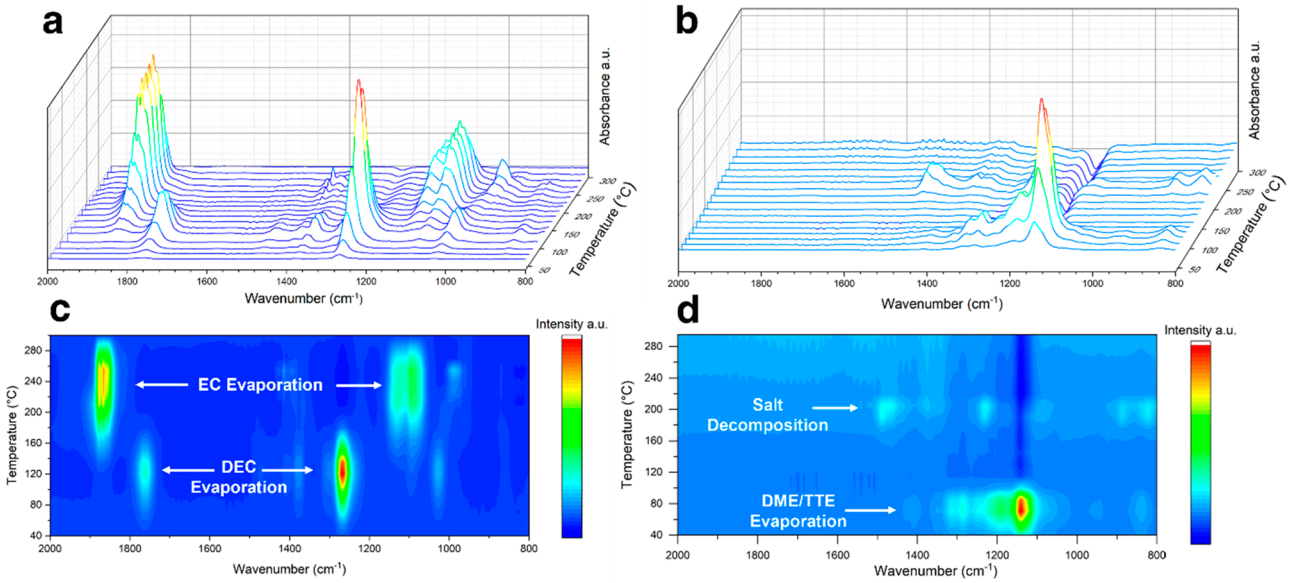

Figure 4. In situ FTIR spectra of (a) plated Li with carbonate and (b) plated Li with LHCE at different temperatures. The 2D intensity mapping of the in situ FTIR spectra of (a) plated Li with carbonate and (b) plated Li with LHCE at different temperatures.

prepared. In both Li-Gr and Li-Si, most heat-absorbing peaks are associated with the evaporation of electrolyte solvents such as DEC and EC (Figure 2a, b; Table S1). No significant heat-releasing peaks exist in the Li-Gr and Li-Si samples when heated to 400 °C. However, when the plated-Li in the carbonate is heated during the DSC measurement, two heat-releasing peaks overlap with the evaporations of DEC and EC solvents, respectively (Figure 2c). When Li melted at around 180 °C, a sharp heat-absorbing peak appeared. The exothermic reactions might be caused by the melted Li quickly reacting with the remaining EC solvent and $LiPF_6$ salt. Figure 2d shows the DSC curves of the plated-Li in LHCE electrolyte. The DME and TTE solvents are mostly evaporated before 100 °C because of the low evaporation points rather than reacting with the Li. A sharp Li melting peak is also shown around 180 °C in Figure 2d, which indicates that the Li was mostly melted rather than oxidized during the heating process. A small oxidation peak can be observed after the complete melting of Li, which is associated with the decomposition of electrolyte salts (details in Figure S2).

The reactivity of the three types of anodes is also studied after 10 cycles. Figure 3a–c shows the DSC curve and the morphology of the lithiated graphite anode after 10 cycles. Similar to the first cycle charged graphite samples, most of the DSC peaks are associated with the evaporation of the electrolyte solvents, with the exception of two exothermic peaks during the solvent evaporation. As shown in Figure 3b,c, there seems to be some SEI accumulation on the graphite surface, as the layered surface morphology of graphite has disappeared after 10 cycles. The small heat releasing peaks (at around 100 and 230 °C) might be associated with the oxidation of the Li-Gr electrode during the solvent evaporation process. A similar trend is found in the 10-cycled Si anode (Figure 3d–f), where two exothermic peaks (at around 100 and 230 °C) are also found during the same temperature range. The SEI accumulation is also obvious on the Si surface (Figure 3e,f). The accumulation of SEI and trapped Li in the Gr and Si electrode after 10 cycles might contribute to the two small heat-releasing peaks observed in the DSC. Overall, the reactivity of lithiated Si and graphite is relatively low, as no large exothermic peaks are observed during the heating process. Figure 3g shows the DSC curve of the plated-Li in the LHCE electrolyte after 10 plate–strip cycles. As the inserted images and SEM images show (Figure 3h,i), because of the superior performance of the LHCE, the deposited Li is still shiny (Figure S1), and the Li particles are bulky after 10 cycles. In addition, most of the electrolyte solvents are evaporated before the Li melting point. As a result, the thermal response of the Li in LHCE is still relatively low, with only 2.25 J/mAh of heat released during the heating process, which is the same magnitude as the Li-Gr and Li-Si cases. However, for the plated-Li in carbonate, there is a large amount of mossy Li accumulated on the electrode surface (Figure 3k,l and inset of Figure 3j). Because of the low cycling Coulombic efficiency (CE) of the carbonate, there is a significant amount of nanosize inactive Li accumulated on the electrode, which can be seen as the mossy Li (Figure 3l).[26] The accumulation of these nanosize inactive Li eventually caused an explosion of the DSC pan during the heating process. These findings correspond to the comments presented by Aurbach and colleagues that cycle number plays a crucial role in the cell safety because the accumulation of inactive Li can be detrimental to the integrity of the cell.[27] Based on the results so far, it can be seen that both the electrolyte and the morphology of Li play significant roles in controlling the reactivity of Li.

In situ FTIR is used to decipher the gas evolution during the DSC of Li metal to study the effects of the electrolyte on the plated-Li. Figure 4a,c shows the FTIR spectra of the gas generated during the heating process of plated-Li with carbonate. Before 130 °C, most of the peaks are associated with the evaporation of DEC (boiling point: 127 °C). The spectra have two main peaks located at 1268 and 1771 cm^{-1}, representing O–C–O symmetric stretch and C=O stretch on the DEC molecules, respectively.[28] EC's evaporation occurs at higher temperatures because of the higher boiling point of 243 °C. The peaks associated with EC are located at 1090 and 1875 cm^{-1}, representing O–C–O asymmetric stretch and

https://doi.org/10.1021/acsenergylett.3c01001
ACS Energy Lett. 2023, 8, 3230–3238

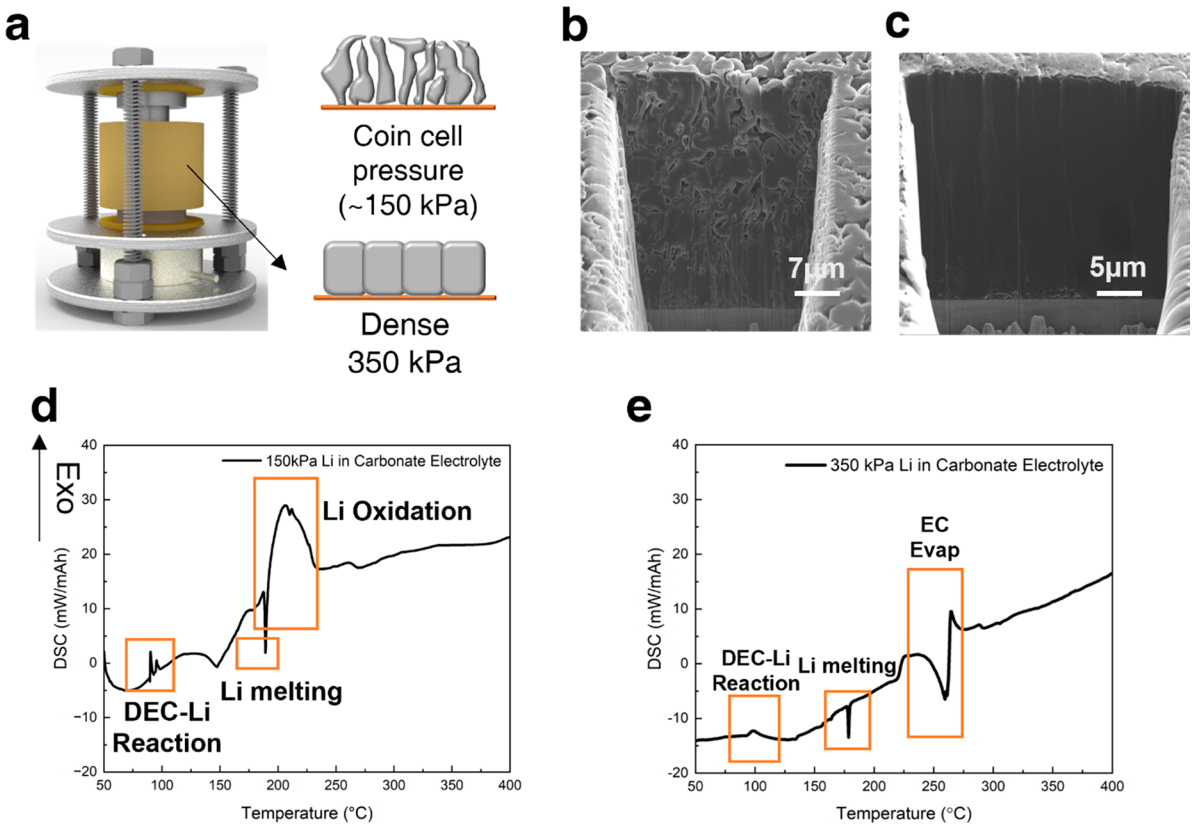

Figure 5. (a) Split cell setup for controlling the stack pressure on Li plating. The cross-sectional morphology of Li plated under (b) 150 kPa stack pressure and (c) 350 kPa stack pressure. DSC curve of Li plated under (d) 150 kPa stack pressure and (e) 350 kPa stack pressure. All Li is plated to 5 mAh/cm^2 at a rate of 0.5 mA/cm^2.

C=O stretch on the EC molecules, respectively.[28] There is no other obvious peak detected during the in situ FTIR study for the plated-Li with carbonate samples. The overlapping temperature ranges between Li melting and solvent boiling can be part of the reasons why the Li shows a large exothermic peak during the DSC measurement (Figure 2c).

Contrary to carbonate, because of the low boiling point of TTE (93.2 °C) and DME (85 °C), the solvents in the LHCE electrolyte evaporated before 120 °C (Figure 4b,d). As a result, the oxidation of Li is caused mainly by the residue organic components and electrolyte salts, as shown by N=O and $C_xH_yF_z^+$ fragment peaks in the FTIR spectrum at 200 °C. The DSC of the pristine LHCE also confirms this observation (Figure S2). The results so far confirm that the electrolyte solvents are the main reasons for the thermal instability of the Li metal cell. However, the future of electrolyte design not only should study the fire-retarding features of the solvents, but also needs to focus on the thermal stability of the electrolyte salts, as the decomposition of electrolyte salt, which leads to the breakage of the S−N bond in the FSI anion to form a FSO2N· radical,[29] will also oxidize the molten Li, interact with the delithiated cathode, and eventually cause the release of heat or even fire.[30]

The effects of Li morphology on Li reactivity are also studied. A split cell setup (Figure 5a) is used to control the morphology of the plated Li by tuning the external stacking pressure.[31] As shown in Figure 5b,c, even with the carbonate electrolyte, which is known for producing Li whiskers, the plated Li can achieve a nearly 100% dense morphology. With the improved morphology, the Li porosity is significantly reduced, as shown in Figure 5e. The plated-Li shows a relatively slow oxidation process instead of a sudden heat release as in Figure 5d. Based on the results, it can be concluded that both the electrolyte and Li morphology play crucial roles in controlling the Li reactivity. Most of the oxidation of Li takes place between Li and electrolyte. If the Li can be plated in a nearly 100% dense morphology, the contact surface area between Li and the electrolyte can be significantly reduced so that the oxidation of Li metal by the electrolyte can also be largely slowed down.

The reactivity of the Li metal full cell is also analyzed. With the knowledge gained so far, we utilized the split cell setup to cycle the Cu||NMC622 full cell with LHCE to achieve uniform Li morphology. After the charging cycle (Figure S3b), the cell is dissembled at 4.4 V, and all the cell components, which includes cathode, anode, and separator, are sealed into an Al pan for DSC measurement. The position of each component is as it is in the full cell setup. Therefore, the insights we obtained from the DSC measurements should be applicable to a real Li metal full cell. Figure 6a shows the DSC curve of delithiated NMC622 with an electrolyte and separator. The delithiated NMC622 will decompose at around 220 and 300 °C to release O_2, which agrees with the literature results.[32] In addition to that, the decomposition of the LiFSI salt is also observed at around 220 °C, which overlaps with the decomposition of NMC622. When the delithiated NMC622 is coupled with plated Li, the released oxygen from the decomposed cathode and LiFSI salt will react with Li violently and cause a huge amount of heat release (Figure 6b). Even if the Li morphology and the electrolyte are optimized, the release of O_2 from the

https://doi.org/10.1021/acsenergylett.3c01001
ACS Energy Lett. 2023, 8, 3230−3238

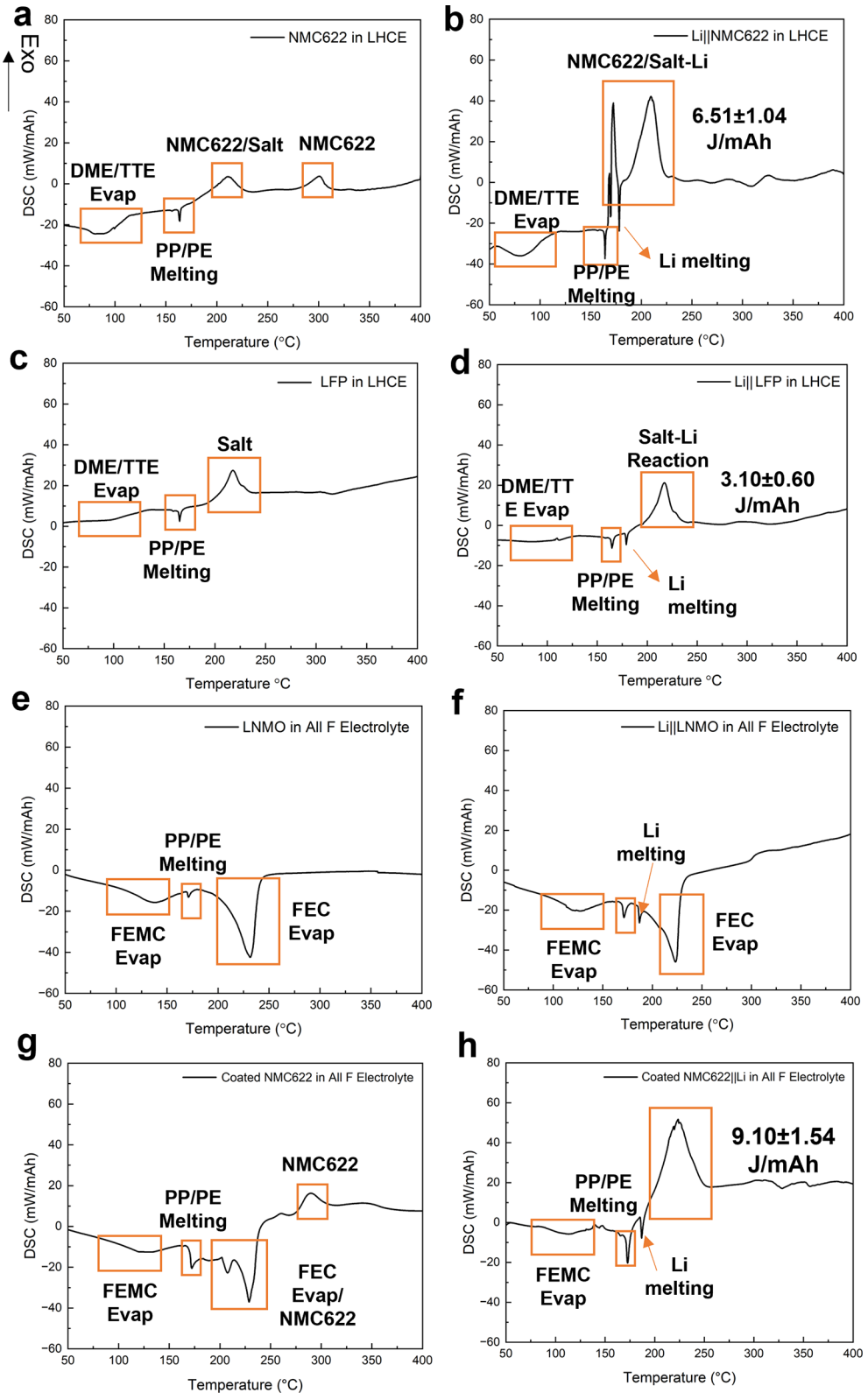

Figure 6. DSC curves of (a) delithiated NMC622 with separator and LHCE; (b) plated Li with delithiated NMC622, separator and LHCE; (c) delithiated LFP with separator and LHCE; (d) plated Li with delithiated LFP, separator and LHCE; (e) delithiated LNMO with separator and All-F electrolyte; (f) plated Li, delithiated LNMO with separator and All-F electrolyte; (g) delithiated coated NMC622 with separator and All-F electrolyte; and (h) plated Li, delithiated coated NMC622 with separator and All-F electrolyte. All cells are cycled at C/20 with corresponding electrolyte.

cathode is still detrimental to full cell level safety. To further evaluate the impact of O_2 on the anode safety, DSC of Li-Gr, Li-Si, and plated Li is done in air (Figure S4). It was found that even though there is limited heat release from Li-Gr at a lower

https://doi.org/10.1021/acsenergylett.3c01001
ACS Energy Lett. 2023, 8, 3230−3238

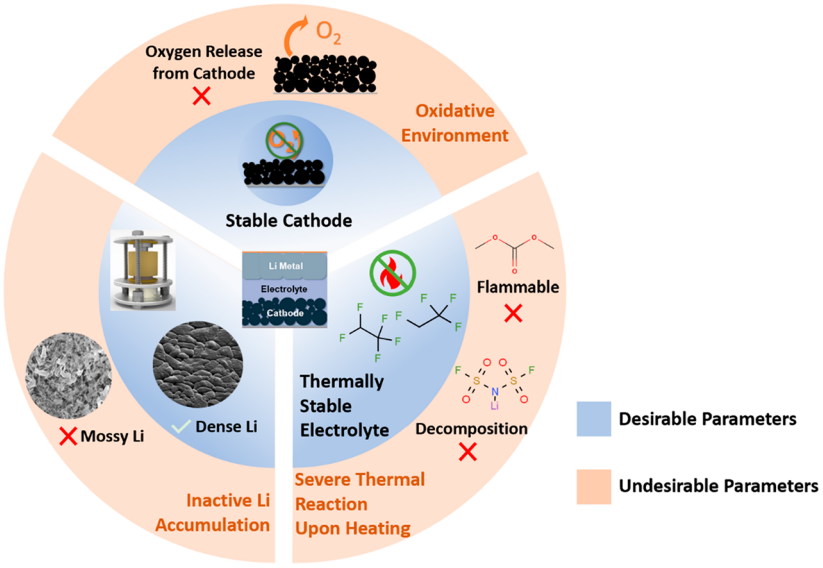

Figure 7. Crucial parameters that control the reactivity of Li metal cells: the inner ring represents the optimized conditions for the Li metal anode, while the outer ring shows the unoptimized conditions.

temperature range (lower than 400 °C), the carbon material started to burn in air because of the presence of O_2. The plated Li shows limited heat release because oxidation of Li in air was rather a slow process. Therefore, no sudden release of heat was observed (Figure S4c). To minimize the impact of the cathode on the Li metal full cell safety, we adopted $LiFePO_4$ (LFP) as the cathode material because of its stability under high temperatures (Figures 6c and S3a). Although there is still some oxidation of Li caused by the decomposition of electrolyte salts (Figure S2), the reduced release of O_2 indeed helps to improve the overall safety of the Li||LFP full cell, which releases only half of the heat as the Li||NMC622 did (Figure 6d). To further minimize the impact from salt decomposition and release of the O_2 from the cathode, the $LiNi_{0.5}Mn_{1.5}O_4$ (LNMO) cathode with all fluorinated electrolyte (All-F electrolyte, 1 M $LiFP_6$ in FEC: Methyl 2,2,2-Trifluoroethyl Carbonate (FEMC), 3:7 by weight) is adopted for this purpose (Figure S3c). As shown in Figure 6e,f, the ultra thermal stability of both the cathode and electrolyte leads to an extraordinarily stable Li metal full cell. There is no obvious release of heat from the DSC test of the Li||LNMO full cell after charging to 4.85 V. The effect of surface coating on the cathode is also investigated in this work (Figure S 3d). A thin layer (~2 nm) of Al_2O_3 is coated onto the NMC622 cathode through an atomic layer deposition (ALD) method.[33] With the applied coating, we hope to stop the interactions between the electrolyte salt and the delithiated cathode to mitigate the decomposition of the cathode.[30] In Figure S6, the thermal stability of the Li||coated NMC622 full cell is tested with LHCE. The DSC shows that even with the Al_2O_3 coating, the thermal stability of the full cell did not improve much. However, it is known so far that the LiFSI salt in the LHCE electrolyte will decompose at around 220 °C, which might contribute to this instability. Therefore, the more stable All-F electrolyte is used in the Li||coated NMC622 full cell to study whether the thermal stability of NMC622 is truly improved or not. As shown in Figure 6g,h, no significant thermal stability improvement is observed in the Al_2O_3 coated-NMC622 sample compared to the uncoated one. The intrinsic instability of delithiated NMC622 will cause the release of O_2 and lead to catastrophic heat generation when coupled with Li.

In conclusion, the reactivities of Li-Gr, Li-Si, and plated Li are compared using integrated DSC and in situ FTIR techniques. It is found that the reactivity of plated Li in the cell is highly related to its morphology and the electrolyte composition (Figure 7). With dense morphology and novel electrolyte, the reactivity of plated Li in the cell can be drastically suppressed to the same level as those of Li-Gr and Li-Si anodes. Therefore, it is crucial to plate Li in a dense morphology to minimize its surface area and utilize thermally stable electrolytes for safe operation of Li metal cells. Moreover, the crosstalk influence from the cathode thermal decomposition may cause a safety hazard when the Li metal anode is used. By switching to more thermally stable cathode materials, such as LFP and LNMO, the thermal stability of the Li metal full cell can be largely improved. In addition, the decomposition of the electrolyte salt also must be strictly controlled. Lastly, the cycle number and cell environment contribute to Li metal reactivity. It is important to control the accumulation of inactive Li and Li morphologies even after extended cycles. The key parameters in controlling the reactivity of Li metal discovered in this work can be applied to the future research of Li metal anodes for practical Li metal full cells.

■ ASSOCIATED CONTENT

Supporting Information

The Supporting Information is available free of charge at https://pubs.acs.org/doi/10.1021/acsenergylett.3c01001.

Detailed descriptions of electrolyte preparations, electrochemical testing, pressure cell setups, Cryo-FIB/SEM operations, ALD coating for NMC622 cathodes, and DSC-FTIR measurements; evaporation temperature of electrolyte solvents; electrochemical curves of anode materials from half cells; DSC of LHCE electrolyte alone; electrochemical curves of cathode materials from anode-free cells; DSC of lithiated anodes in air; DSC of delithiated LFP in LHCE; DSC of delithiated coated NMC622 in LHCE (PDF)

https://doi.org/10.1021/acsenergylett.3c01001
ACS Energy Lett. 2023, 8, 3230−3238

AUTHOR INFORMATION

Corresponding Authors

Wurigumula Bao − *Pritzker School of Molecular Engineering, University of Chicago, Chicago, Illinois 60637, United States;* orcid.org/0000-0001-8109-1546; Email: wubao@uchicago.edu

Ying Shirley Meng − *Department of NanoEngineering, University of California, San Diego, La Jolla, California 92093, United States; Pritzker School of Molecular Engineering, University of Chicago, Chicago, Illinois 60637, United States;* orcid.org/0000-0001-8936-8845; Email: shirleymeng@uchicago.edu

Authors

Bingyu Lu − *Department of NanoEngineering, University of California, San Diego, La Jolla, California 92093, United States*

Diyi Cheng − *Materials Science and Engineering Program, University of California, San Diego, La Jolla, California 92093, United States;* orcid.org/0000-0003-1616-9209

Bhagath Sreenarayanan − *Department of NanoEngineering, University of California, San Diego, La Jolla, California 92093, United States*

Weikang Li − *Department of NanoEngineering, University of California, San Diego, La Jolla, California 92093, United States*

Bhargav Bhamwala − *Department of NanoEngineering, University of California, San Diego, La Jolla, California 92093, United States*

Complete contact information is available at: https://pubs.acs.org/10.1021/acsenergylett.3c01001

Funding

This work was supported by the Office of Vehicle Technologies of the U.S. Department of Energy through the Advanced Battery Materials Research (BMR) Program (Battery500 Consortium) under Contract DE-EE0007764. Cryo-FIB was performed at the San Diego Nanotechnology Infrastructure (SDNI), a member of the National Nanotechnology Coordinated Infrastructure, which is supported by the National Science Foundation (Grant ECCS-1542148). We acknowledge the UC Irvine Materials Research Institute (IMRI) for the use of the DSC-FTIR, funded in part by the National Science Foundation Major Research Instrumentation Program under Grant CHE-1338173. The authors would like to acknowledge Neware Technology Limited for the donation of BTS4000 cyclers which are used for testing the cells in this work.

Notes

The authors declare no competing financial interest.

REFERENCES

(1) Xu, W.; Wang, J.; Ding, F.; Chen, X.; Nasybulin, E.; Zhang, Y.; Zhang, J.-G. Lithium Metal Anodes for Rechargeable Batteries. *Energy Environ. Sci.* **2014**, *7* (2), 513−537.

(2) Liu, J.; Bao, Z.; Cui, Y.; Dufek, E. J.; Goodenough, J. B.; Khalifah, P.; Li, Q.; Liaw, B. Y.; Liu, P.; Manthiram, A.; Meng, Y. S.; Subramanian, V. R.; Toney, M. F.; Viswanathan, V. V.; Whittingham, M. S.; Xiao, J.; Xu, W.; Yang, J.; Yang, X. Q.; Zhang, J. G. Pathways for Practical High-Energy Long-Cycling Lithium Metal Batteries. *Nat. Energy* **2019**, *4*, 180−186.

(3) Fang, C.; Wang, X.; Meng, Y. S. Key Issues Hindering a Practical Lithium-Metal Anode. *Trends Chem.* **2019**, *1* (2), 152−158.

(4) Niu, C.; Pan, H.; Xu, W.; Xiao, J.; Zhang, J. G.; Luo, L.; Wang, C.; Mei, D.; Meng, J.; Wang, X.; Liu, Z.; Mai, L.; Liu, J. Self-Smoothing Anode for Achieving High-Energy Lithium Metal Batteries under Realistic Conditions. *Nat. Nanotechnol.* **2019**, *14*, 594−601.

(5) Weber, R.; Genovese, M.; Louli, A. J.; Hames, S.; Martin, C.; Hill, I. G.; Dahn, J. R. Long Cycle Life and Dendrite-Free Lithium Morphology in Anode-Free Lithium Pouch Cells Enabled by a Dual-Salt Liquid Electrolyte. *Nat. Energy* **2019**, *4*, 683−689.

(6) Louli, A. J.; Eldesoky, A.; Weber, R.; Genovese, M.; Coon, M.; deGooyer, J.; Deng, Z.; White, R. T.; Lee, J.; Rodgers, T.; Petibon, R.; Hy, S.; Cheng, S. J. H.; Dahn, J. R. Diagnosing and Correcting Anode-Free Cell Failure via Electrolyte and Morphological Analysis. *Nat. Energy* **2020**, *5* (9), 693−702.

(7) Tobishima, S.; Sakurai, Y.; Yamaki, J. Safety Characteristics of Rechargeable Lithium Metal Cells. *J. Power Sources* **1997**, *68* (2), 455−458.

(8) Yamaki, J. I.; Tobishima, S. I.; Sakurai, Y.; Saito, K. I.; Hayashi, K. Safety Evaluation of Rechargeable Cells with Lithium Metal Anodes and Amorphous V2O5 Cathodes. *J. Appl. Electrochem.* **1997**, *28* (2), 135−140.

(9) Zuckerbrod, D.; Giovannoni, R. T.; Grossman, K. R. Life, performance and safety of Grace rechargeable lithium-titanium disulfide cells. *Proceedings of the 34th International Power Sources Symposium* **1990**, 172−175.

(10) Hess, S.; Wohlfahrt-Mehrens, M.; Wachtler, M. Flammability of Li-Ion Battery Electrolytes: Flash Point and Self-Extinguishing Time Measurements. *J. Electrochem. Soc.* **2015**, *162* (2), A3084−A3097.

(11) Nagasubramanian, G.; Fenton, K. Reducing Li-Ion Safety Hazards through Use of Non-Flammable Solvents and Recent Work at Sandia National Laboratories. *Electrochim. Acta* **2013**, *101*, 3−10.

(12) Choi, N. S.; Profatilova, I. A.; Kim, S. S.; Song, E. H. Thermal Reactions of Lithiated Graphite Anode in LiPF6-Based Electrolyte. *Thermochim. Acta* **2008**, *480* (1−2), 10−14.

(13) Kriston, A.; Pfrang, A.; Döring, H.; Fritsch, B.; Ruiz, V.; Adanouj, I.; Kosmidou, T.; Ungeheuer, J.; Boon-Brett, L. External Short Circuit Performance of Graphite-LiNi1/3Co1/3Mn1/3O2 and Graphite-LiNi0.8Co0.15Al0.05O2 Cells at Different External Resistances. *J. Power Sources* **2017**, *361*, 170−181.

(14) Jiang, J.; Dahn, J. R. Effects of Solvents and Salts on the Thermal Stability of LiC6. *Electrochim. Acta* **2004**, *49* (26), 4599−4604.

(15) Golubkov, A. W.; Fuchs, D.; Wagner, J.; Wiltsche, H.; Stangl, C.; Fauler, G.; Voitic, G.; Thaler, A.; Hacker, V. Thermal-Runaway Experiments on Consumer Li-Ion Batteries with Metal-Oxide and Olivin-Type Cathodes. *RSC Adv.* **2014**, *4* (7), 3633−3642.

(16) Andersson, A. M.; Edström, K.; Thomas, J. O. Characterisation of the Ambient and Elevated Temperature Performance of a Graphite Electrode. *J. Power Sources* **1999**, *81*−*82*, 8−12.

(17) Galushkin, N. E.; Yazvinskaya, N. N.; Galushkin, D. N. Mechanism of Gases Generation during Lithium-Ion Batteries Cycling. *J. Electrochem. Soc.* **2019**, *166* (6), A897−A908.

(18) Puthusseri, D.; Parmananda, M.; Mukherjee, P. P.; Pol, V. G. Probing the Thermal Safety of Li Metal Batteries. *J. Electrochem. Soc.* **2020**, *167* (12), 120513.

(19) Liu, D. H.; Bai, Z.; Li, M.; Yu, A.; Luo, D.; Liu, W.; Yang, L.; Lu, J.; Amine, K.; Chen, Z. Developing High Safety Li-Metal Anodes for Future High-Energy Li-Metal Batteries: Strategies and Perspectives. *Chem. Soc. Rev.* **2020**, *49* (15), 5407−5445.

(20) Wu, L.; Song, Z.; Liu, L.; Guo, X.; Kong, L.; Zhan, H.; Zhou, Y.; Li, Z. A New Phosphate-Based Nonflammable Electrolyte Solvent for Li-Ion Batteries. *J. Power Sources* **2009**, *188* (2), 570−573.

(21) Zeng, Z.; Wu, B.; Xiao, L.; Jiang, X.; Chen, Y.; Ai, X.; Yang, H.; Cao, Y. Safer Lithium Ion Batteries Based on Nonflammable Electrolyte. *J. Power Sources* **2015**, *279*, 6−12.

(22) Yin, Y.; Yang, Y.; Cheng, D.; Mayer, M.; Holoubek, J.; Li, W.; Raghavendran, G.; Liu, A.; Lu, B.; Davies, D. M.; Chen, Z.; Borodin, O.; Meng, Y. S. Fire-Extinguishing, Recyclable Liquefied Gas Electrolytes for Temperature-Resilient Lithium-Metal Batteries. *Nature Energy* **2022**, *7*, 548−559.

(23) Cao, X.; Xu, Y.; Zhang, L.; Engelhard, M. H.; Zhong, L.; Ren, X.; Jia, H.; Liu, B.; Niu, C.; Matthews, B. E.; Wu, H.; Arey, B. W.; Wang, C.; Zhang, J. G.; Xu, W. Nonflammable Electrolytes for Lithium Ion Batteries Enabled by Ultraconformal Passivation Interphases. *ACS Energy Lett.* **2019**, *4* (10), 2529−2534.
(24) Fan, X.; Ji, X.; Chen, L.; Chen, J.; Deng, T.; Han, F.; Yue, J.; Piao, N.; Wang, R.; Zhou, X.; Xiao, X.; Chen, L.; Wang, C. All-Temperature Batteries Enabled by Fluorinated Electrolytes with Non-Polar Solvents. *Nat. Energy* **2019**, *4* (10), 882−890.
(25) Laing, M. Melting Point, Density, and Reactivity of Metals. *J. Chem. Educ.* **2001**, *78* (8), 1054.
(26) Fang, C.; Li, J.; Zhang, M.; Zhang, Y.; Yang, F.; Lee, J. Z.; Lee, M.; Alvarado, J.; Schroeder, M. A.; Yang, Y.; Lu, B.; Williams, N.; Ceja, M.; Yang, L.; Cai, M.; Gu, J.; Xu, K.; Wang, X.; Meng, Y. S. Quantifying inactive lithium in lithium metal batteries. *Nature* **2019**, *572*, 511−515.
(27) Dan, P.; Mengeritski, E.; Geronov, Y.; Aurbach, D.; Weisman, I. Performances and Safety Behaviour of Rechargeable AA-Size Li/LixMnO2 Cell. *J. Power Sources* **1995**, *54* (1), 143−145.
(28) Shi, F.; Ross, P. N.; Somorjai, G. A.; Komvopoulos, K. The Chemistry of Electrolyte Reduction on Silicon Electrodes Revealed by in Situ ATR-FTIR Spectroscopy. *J. Phys. Chem. C* **2017**, *121* (27), 14476−14483.
(29) Huang, J.; Hollenkamp, A. F. Thermal Behavior of Ionic Liquids Containing the FSI Anion and the Li Cation. *J. Phys. Chem. C* **2010**, *114*, 21840−21847.
(30) Jia, H.; Yang, Z.; Xu, Y.; Gao, P.; Zhong, L.; Kautz, D. J.; Wu, D.; Fliegler, B.; Engelhard, M. H.; Matthews, B. E.; Broekhuis, B.; Cao, X.; Fan, J.; Wang, C.; Lin, F.; Xu, W. Is Nonflammability of Electrolyte Overrated in the Overall Safety Performance of Lithium Ion Batteries? A Sobering Revelation from a Completely Nonflammable Electrolyte. *Adv. Energy Mater.* **2023**, *13*, 2203144.
(31) Fang, C.; Lu, B.; Pawar, G.; Zhang, M.; Cheng, D.; Chen, S.; Ceja, M.; Doux, J.-M.; Musrock, H.; Cai, M.; Liaw, B.; Meng, Y. S. Pressure-Tailored Lithium Deposition and Dissolution in Lithium Metal Batteries. *Nat. Energy* **2021**, *6*, 987−994.
(32) Julien, C. M.; Mauger, A.; Zaghib, K.; Groult, H. Comparative Issues of Cathode Materials for Li-Ion Batteries. *Inorganics* **2014**, *2* (1), 132−154.
(33) Li, W.; Cheng, D.; Shimizu, R.; Li, Y.; Yao, W.; Raghavendran, G.; Zhang, M.; Meng, Y. S. Artificial Cathode Electrolyte Interphase for Improving High Voltage Cycling Stability of Thick Electrode with Co-Free 5 V Spinel Oxides. *Energy Storage Mater.* **2022**, *49*, 77−84.

https://doi.org/10.1021/acsenergylett.3c01001
ACS Energy Lett. 2023, 8, 3230−3238